

RSC Advances

Supporting Information

Metallo-ions Linked Surface-Confining Molecular Dyads of Zn-Porphyrin-Metallo-Terpyridine: Experimental and Theoretical Study

Bhawna Gera,^a Arun Kumar Manna^b and Prakash Chandra Mondal^{*a,c}

^aDepartment of Chemistry, University of Delhi, Delhi-110007, India

^bDepartment of Materials and Interfaces, Weizmann Institute of Science, Rehovot, Israel

^cPresent address: National Institute for Nanotechnology, University of Alberta, Edmonton, Edmonton, AB, T6G 2M9 Canada

E-mail: mondalpc@gmail.com (P.C.M)

Materials and Methods (for characterization)

¹H and ¹³C NMR spectra were recorded with JEOL 400 NMR spectrometer (Model No. JNMECX 400P recorded at Delhi University, Central Instrumentation Facility).

FT-IR spectra (KBr pellets) were recorded with a Perkin Elmer spectrometer in a range of 400–4000 cm⁻¹, (Delhi University, Departmental facility).

UV-vis spectra were recorded using JASCO UV-Vis-NIR (Model No. V670).

Fluorescence spectra on silicon substrates were recorded using Perkin Elmer (LS45 Perkin-Elmer FT-IR Spectrometer. Mass Spectra were recorded on THERMO Finnigan LCQ Advantage max ion trap Spectrometer (MSAIF, CDRI, Lucknow, India).

Atomic Force Microscopy was recorded using an NT-MD instrument. AFM images were recorded on silicon substrates in tapping/semicontact mode in air. Aluminium-coated cantilevers with silicon nitride tips whose resonance frequency was 70-90 kHz used for the topography measurements. The spring constant of the cantilever tip (k) used was 0.3 N/m and the topography images were recorded at a scan rate of 0.5 Hz. Deflection set point was fixed at 0.75 V. Aspect ratio, integral gain, proportional gain were fixed at 1.00, 0.2, 0.4, respectively. Samples/lines was at 512. In order to confirm consistency and reproducibility of the results, several images of each sample were recorded at different positions. Average root-mean square roughness values were estimated from 4 different measurements.

Synthesis of 4'-pyridyl terpyridyl (4'-pytpy):

4'-pyridyl-2,2':6',2''-terpyridine (4'-pytpy) was synthesized following published procedure^[S1] and needle shape white crystals were obtained. The ligand was characterized by ¹H, ¹H-¹H COSY, ¹³C NMR, elemental analysis, UV-vis and ESI-MS data: δ_H (400 MHz, CDCl₃), δ/ppm: 8.76 (s, 2H, Ar H), 8.78 (d, *J* = 8.6Hz, 2H), 8.68 (d, *J* = 8.05Hz, 2H), 7.8 (d, *J* = 8.4Hz, 2H), 7.89 (t, *J* = 6.8Hz, 2H), 8.75 (d, *J* = 8.2Hz, 2H), 7.39 (t, *J* = 6.72, 2H). ¹³C NMR (100 MHz, CDCl₃), δ/ppm: 118.51, 121.27, 121.59, 124.03, 136.88, 145.83, 147.29, 149.09, 150.44, 155.57, 156.25. EI-MS; *m/z* (%): 310 (100) (M⁺). Anal. Calcd for C₂₀H₁₄N₄: C, 77.1; H, 4.8; N, 18.02. Found: C, 76.5; H, 4.40; N, 17.89. UV-vis λ_{max}/nm (ε/10³ dm³ mol⁻¹ cm⁻¹): 254 (8.02).

Synthesis of Fe-PT, Ru-PT and Os-PT:

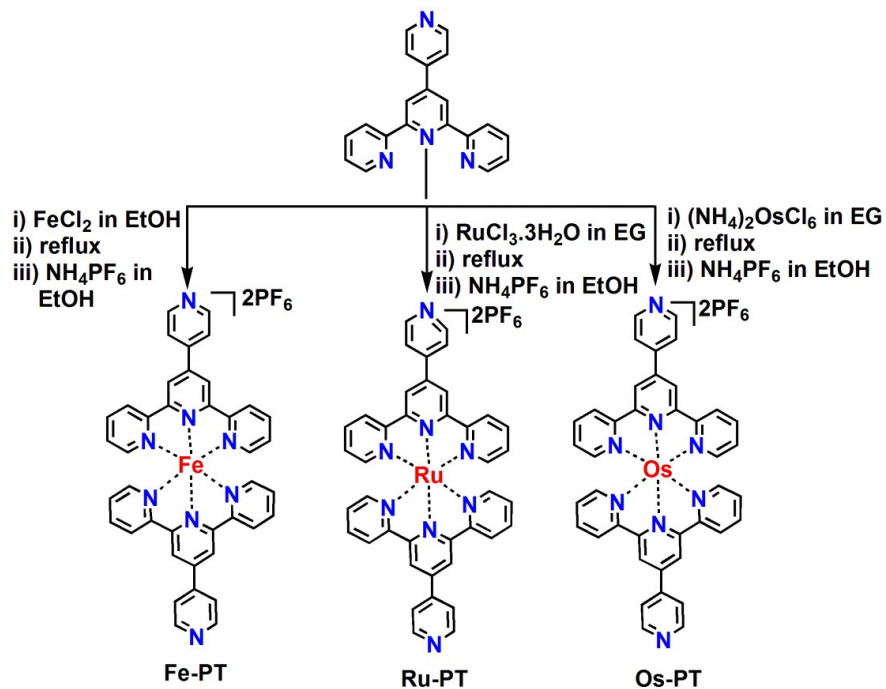
The Fe-PT, Ru-PT and Os-PT complexes were prepared via published method^[S2] (**Scheme S1**). The complexes were characterized by the help of ¹H and ¹H-¹H COSY, ¹³C NMR, ESI mass, FTIR, elemental analysis, UV-vis spectroscopy and cyclic voltammetry (CV).

Characterization data:

Fe-PT: ^1H NMR (400 MHz, CD₃CN); δ /ppm: 9.20 (s, Ar, 4H), 9.02 (d, J = 8.0 Hz, 4H), 8.61 (d, J = 11 Hz, 4H), 8.23 (d, J = 10.2 Hz, 4H), 7.90 (t, J = 8.2 Hz, 4H), 7.15 (d, J = 5.8 Hz, 4H), 7.10 (t, J = 7 Hz, 4H). ^{13}C NMR (100 MHz, CD₃CN), δ /ppm: 118.29, 122.58, 122.98, 125.04, 128.36, 139.82, 148.75, 152.08, 154.22, 158.77, 161.84. EI-MS; m/z (%): 338 (90) [M-2PF₆]²⁺, 339 (46) [(M-2PF₆)+H⁺]²⁺, 821 (30) [(M-PF₆)]⁺. UV-vis (CH₃CN) λ_{max} /nm ($\varepsilon/10^3$ dm³ mol⁻¹ cm⁻¹): 569 (23.00). FT-IR, KBr (cm⁻¹): 838 (vs), 1408 (m) and 1598 (m). Anal. Calcd for C₄₀H₂₈N₈FeP₂F₁₂: C, 45.47; H, 3.63; N, 10.61. Found: C, 45.16; H, 3.34; N, 9.96%.

Ru-PT: ^1H NMR (400 MHz, CD₃CN) δ /ppm: 9.03 (s, Ar, 4H), 8.95 (d, J = 6.2 Hz, 4H), 8.65 (d, J = 9 Hz, 4H), 8.11 (d, J = 6.2 Hz, 4H), 7.96 (t, J = 8 Hz, 4H), 7.40 (d, J = 6Hz, 4H), 7.18 (t, J = 6 Hz, 4H). ^{13}C NMR (100 MHz, CD₃CN), δ /ppm: 118.28, 122.79, 122.86, 125.69, 128.68, 139.09, 146.42, 152.20, 153.36, 156.66, 158.84. EI-MS; m/z (%): 361 (45) [M-2PF₆]²⁺, 362 (60) [(M-2PF₆)+H⁺]²⁺. UV-vis (CH₃CN) λ_{max} /nm ($\varepsilon/10^3$ dm³ mol⁻¹ cm⁻¹): 490 (29.77). FT-IR, KBr (cm⁻¹): 839 (vs), 1408 (m) and 1600 (m). Anal. Calcd for C₄₀H₂₈N₈RuP₂F₁₂: C, 47.49; H, 2.79; N, 11.08. Found: C, 47.83; H, 3.12; N, 11.28%.

Os-PT: ^1H NMR (400 MHz, CD₃CN) δ /ppm: 9.06 (s, Ar, 4H), 8.96 (d, J = 6.8 Hz, 4H), 8.65 (d, J = 8.5 Hz, 4H), 8.14 (d, J = 7 Hz, 4H), 7.84 (t, J = 8.4 Hz, 4H), 7.29 (d, J = 6.2Hz, 4H), 7.14 (t, J = 7.5 Hz, 4H). ^{13}C NMR (100 MHz, CD₃CN), δ /ppm: 118.28, 122.79, 122.86, 125.69, 128.68, 139.09, 146.42, 152.20, 153.36, 156.66, 158.84. EI-MS m/z (%): 405 (78) [M-2PF₆]²⁺, 406 (100) [(M-2PF₆)+H⁺]²⁺. UV-vis (CH₃CN) λ_{max} /nm ($\varepsilon/10^3$ dm³ mol⁻¹ cm⁻¹): 490 (27.45), 674 (8.020). FT-IR, KBr (cm⁻¹): 836 (vs), 1406 (m) and 1596 (m). Anal. Calcd for C₄₀H₂₈N₈OsP₂F₁₂: C, 43.64; H, 2.85; N, 10.18. Found: C, 42.83; H, 2.85; N, 10.01%.



Scheme S1. Scheme for the preparation of Fe-PT, Ru-PT and Os-PT (metallo-ligands).

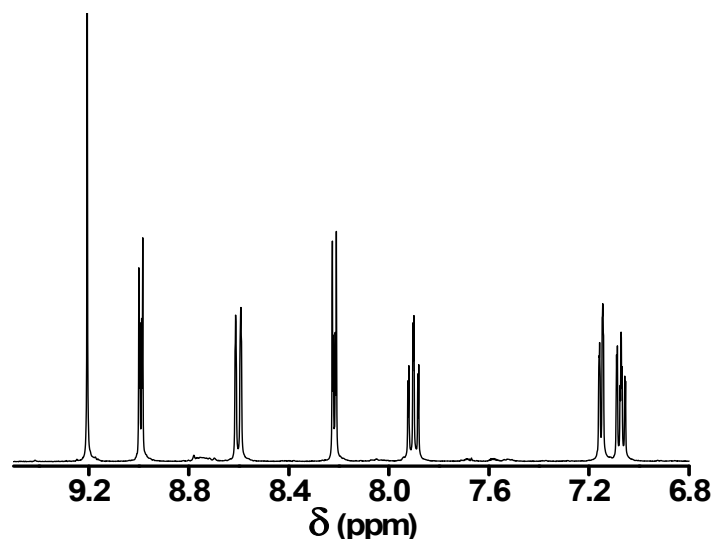


Fig. S1a. ^1H NMR spectrum of Fe-PT in CD_3CN .

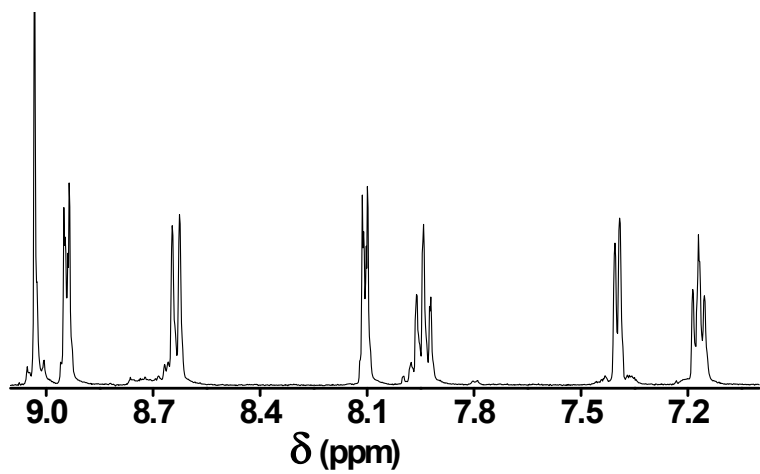


Fig. S1b. ^1H NMR spectrum of Ru-PT in CD_3CN .

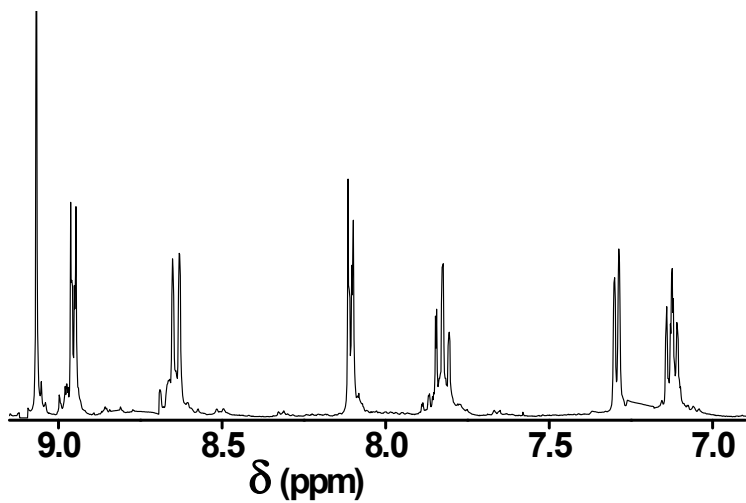


Fig. S1c. ^1H NMR spectrum of Os-PT in CD_3CN .

Synthesis of tetrakis(4-pyridyl)-porphyrin {[H₂T(4-Py)P]}: Synthesis of the ligands was carried out according to the existing literature procedure.^[S3]

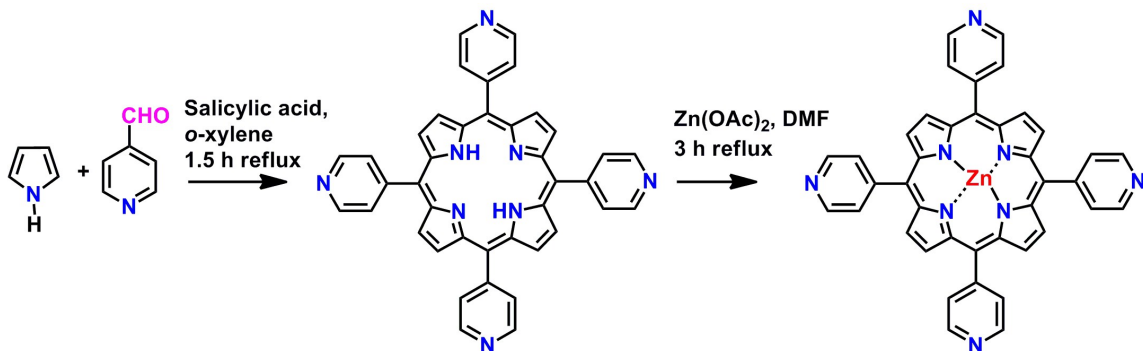
Characterization data:

H₂T(4-Py)P: $^1\text{H-NMR}$ (CDCl_3 , 400MHz) $\delta = 9.1$ (d), $\delta = 8.9$ (s), $\delta = 8.2$ (d), $\delta = -2.9$ (s) ppm. UV-vis (CHCl_3) λ_{max} : 416 (s, Soret band), 512 (w, Q band), 546 (w, Q band), 589 (w, Q

band), 646 (w, Q band) nm. TPyP (3): $^1\text{H-NMR}$ (CDCl_3 , 400 MHz) δ = 9.4 (s), 9.0 (d), 8.8 (s), -2.9 (s) ppm.

Synthesis of Zn-TPyP: Synthesis of the Zn-TPyP was carried out via published method^[S4].
Characterization data:

UV-vis (CHCl_3) λ_{max} : ZnTPyP(4) : 421(s, Soret band), 551 (w, Q band). Mass spectra: 682 m/e.



Scheme S2. Scheme for the preparation of TPyP and Zn-TPyP complex (metallo-ligands).

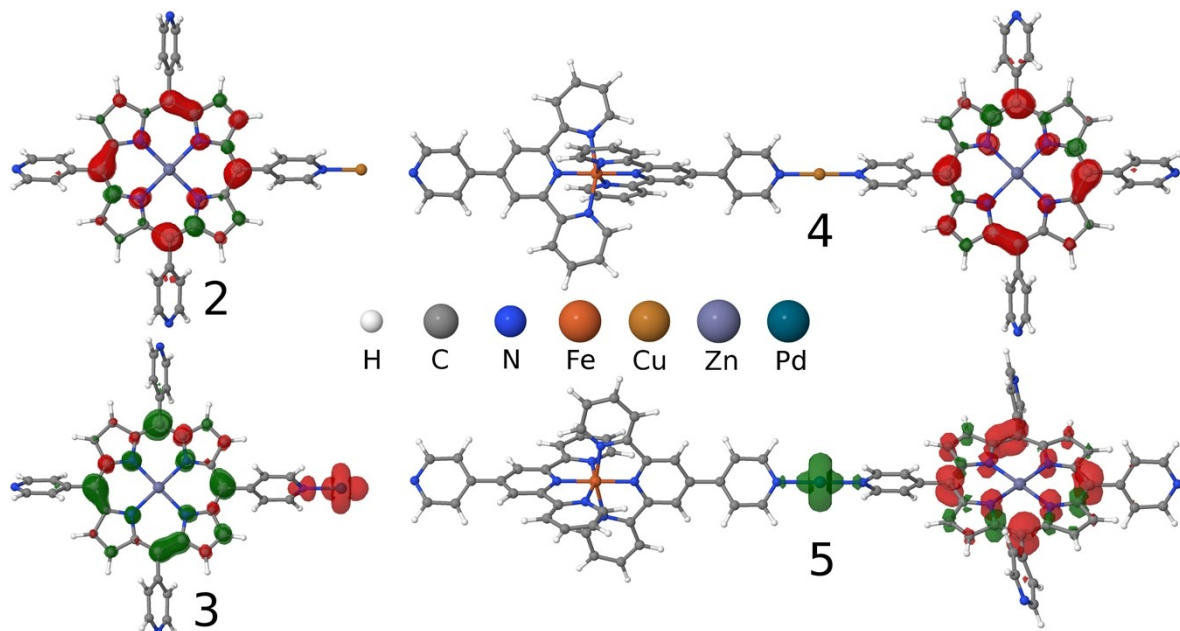


Figure S2. Spin density distribution of the complex 2, 3, 4 and 5 as calculated by using ωB97XD XC functional with 6-31+G(d,p) basis set for light atoms and LANL2DZ basis set for metals with ECP for the core electrons.

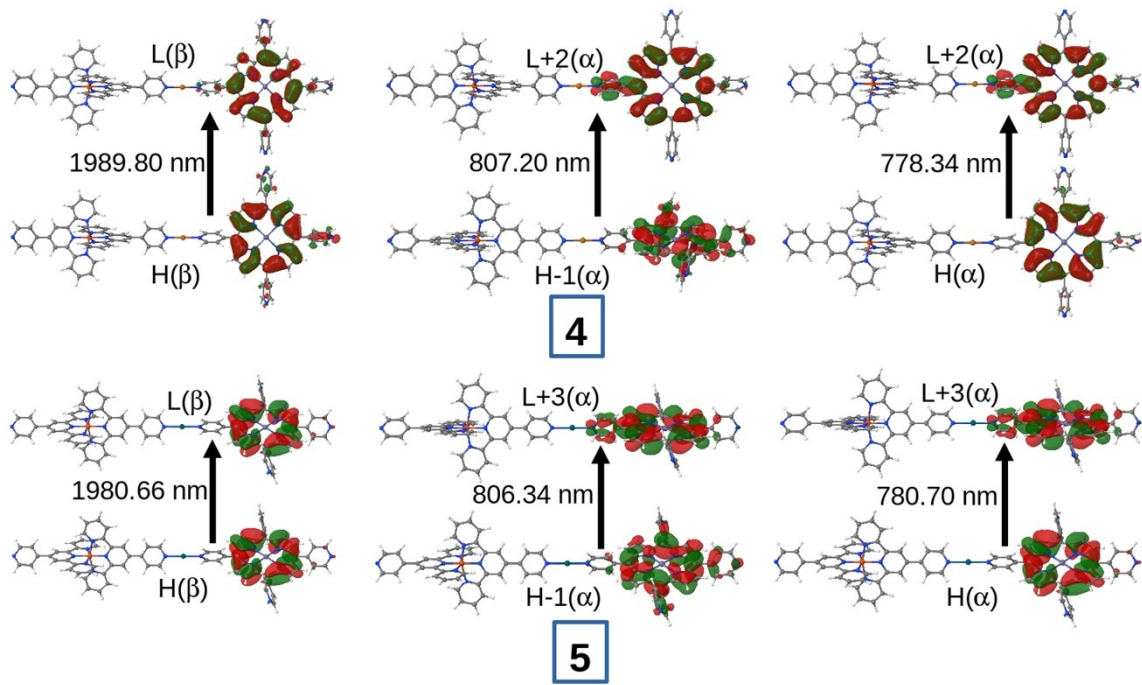


Figure S3. Low-lying electronic excitations with relevant frontier molecular orbitals for the complex 4 and 5 as calculated by using ω B97XD XC functional with 6-31+G(d,p) basis set for light atoms and LANL2DZ basis set for metals with ECP for the core electrons. H and L stand for HOMO and LUMO, respectively. α and β refer the alpha and beta set of spin-orbitals, respectively.

Table S1. HOMO-LUMO gaps (ΔE_{H-L}) for five complexes (1, 2, 3, 4 and 5) in gas phase calculated by using DFT employing different XC functionals (ω B97XD, CAM-B3LYP and B3LYP) with 6-31+G(d,p) basis set for light atoms and LANL2DZ basis set for metals with ECP for the core electrons.

Complex	ΔE_{H-L} (eV) / ω B97XD	ΔE_{H-L} (eV) / CAM-B3LYP	ΔE_{H-L} (eV) / B3LYP
1	5.62 (α), 5.62 (β)	4.64 (α), 4.64 (β)	2.85 (α), 2.85 (β)
2	5.35 (α), 4.45 (β)	4.01 (α), 3.40 (β)	1.82 (α), 1.28 (β)
3	4.44 (α), 3.96 (β)	3.40 (α), 2.89 (β)	1.27 (α), 0.41 (β)
4	4.64 (α), 4.44 (β)	3.56 (α), 3.40 (β)	1.53 (α), 1.16 (β)
5	4.07 (α), 4.44 (β)	3.04 (α), 3.40 (β)	0.52 (α), 1.17 (β)

Table S2. TDDFT excitation energy for all five complexes (1, 2, 3, 4 and 5) computed in gas phase using different XC functionals employing 6-31+G(d,p) basis set for light atoms and LANL2DZ basis for metals with ECP for the core electrons. Values within bracket represent

oscillator strengths for each excitation. Significant molecular orbital replacements associated with each electronic excitation are also listed.

Complex	Excitation Energy (nm)/ ω B97XD	Excitation Energy (nm)/ CAM-B3LYP	Excitation Energy (nm)/ B3LYP	Experimental (nm)
1 [HOMO=166 (α)/166(β)]	559.89 (0.0032) H → L; H-1 → L+1 559.89 (0.0031) H → L+1; H-1 → L 361.72 (1.4826) H→L; H-1→ L+1 361.72 (1.4822) H-1→L; H→ L+1	547.97 (0.0023) H → L; H-1 → L+1 547.97 (0.0023) H → L+1; H-1 → L 362.78 (1.4885) H→L; H-1→ L+1 362.78 (1.4880) H-1→L; H→ L+1	538.91 (0.0067) H → L; H-1 → L+1 538.91 (0.0066) H → L+1; H-1 → L 380.47 (1.2996) H→L; H-1→ L+1 380.47 (1.2992) H-1→L; H→ L+1	560 (Q-band), 442 (B-band)
2 [HOMO=175 (α)/174(β)]	2012.24 (0.0004) H(β)→L(β) 810.06 (0.0170) H-1(α)→L(α) 781.26 (0.0350) H-1(α)→L+2(α) 622.15 (0.0046) H(α)→L(α) 606.75 (0.0026) H-9(β)→L(β) 428.79 (0.1445) H-7(β)→L(β) 404.38 (0.3671) H-8(β)→L(β) 354.45 (0.6501) H(β)→L+2(β)	2090.45 (0.0004) H(β)→L(β) 808.03 (0.0164) H-1(α)→L(α) 778.40 (0.0320) H-1(α)→L+2(α) 626.59 (0.0050) H(α)→L(α) 616.56 (0.0020) H-9(β)→L(β) 447.80 (0.1245) H-7(β)→L(β) 423.27 (0.2677) H-8(β)→L(β) 363.33 (0.8274) H(β)→L+2(β)	998.59 (0.0022) H-4(β)→L(β) 908.67 (0.0049) H-5(β)→L(β) 813.20 (0.0006) H(α)→L(α) 801.57 (0.0034) H-7(β)→L(β) 772.96 (0.0038) H-1(α)→L+2(α) H-8(β)→L(β) 726.37 (0.0090) H-9(β)→L(β) 626.59 (0.0050) H(α)→L(α) 685.14 (0.0308) H-10(β)→L(β) 634.07 (0.0391) H(α)→L+2(α) 578.43 (0.0637) H(α)→L+2(α)	433
3 [HOMO=174 (α)/174(β)]	2020.21 (0.0002) H(α)→L(α) 803.76 (0.0158) H-1(β)→L+1(β) 778.93 (0.0333) H(β)→L+1(β) 622.48 (0.0039) H(β)→L+1(β)	2090.56 (0.0002) H(α)→L(α) 802.51 (0.0152) H-1(β)→L+1(β) 777.52 (0.0302) H(β)→L+1(β) 626.66 (0.0044) H(β)→L+1(β)	1010.15 (0.0022) H-4(α)→L(α) 913.97 (0.0034) H-5(α)→L(α) 803.19 (0.0032) H-7(α)→L(α) 778.47 (0.0029) H-8(α)→L(α)	448

	606.52 (0.0022) H(β) \rightarrow L+2(β) 428.76 (0.1692) H-1(α) \rightarrow L(α) 405.10 (0.3510) H-8(α) \rightarrow L(α) 354.43 (0.6776) H(α) \rightarrow L+2(α)	616.87 (0.0012) H(β) \rightarrow L+2(β) 447.80 (0.1482) H-7(α) \rightarrow L(α) 424.12 (0.2427) H-8(α) \rightarrow L(α) 362.85 (0.7611) H(α) \rightarrow L+2(α)	725.66 (0.0087) H-9(β) \rightarrow L(β) 685.33 (0.0299) H-10(β) \rightarrow L(β) 674.07 (0.0068) H(β) \rightarrow L+2(β)	
4 [HOMO=344 (α)/343(β)]	1989.80 (0.0005) H(β) \rightarrow L(β) 807.20 (0.0156) H-1(α) \rightarrow L+2(α) 778.34 (0.0369) H(α) \rightarrow L+2(α)	2064.55 (0.0005) H(β) \rightarrow L(β) 806.37 (0.0157) H-1(α) \rightarrow L+2(α) 776.10 (0.0329) H(α) \rightarrow L+2(α)	2698.36 (0.0002) H-1(β) \rightarrow L(β) 1708.78 (0.0009) H(β) \rightarrow L(β) 1270.57 (0.0009) H-2(β) \rightarrow L(β) 1218.87 (0.0003) H-3(β) \rightarrow L(β) 1105.01 (0.0023) H-4(β) \rightarrow L(β) 915.43 (0.0001) H(α) \rightarrow L(α)	579
5 [HOMO=343 (α)/343(β)]	1980.66 (0.0004) H(β) \rightarrow L(β) 806.34 (0.0158) H-1(α) \rightarrow L+3(α) 780.70 (0.0358) H(α) \rightarrow L+3(α); H-1(α) \rightarrow L+5(α)	2049.14 (0.0005) H(β) \rightarrow L(β) 805.23 (0.0161) H-1(α) \rightarrow L+3(α) 777.62 (0.0316) H(α) \rightarrow L+3(α); H-1(α) \rightarrow L+5(α)	5450.17 (0.0014) H(α) \rightarrow L(α) 2688.94 (0.0001) H-1(β) \rightarrow L(β) 2491.79 (0.0002) H-2(α) \rightarrow L(α) 1683.95 (0.0009) H(β) \rightarrow L(β) 1259.69 (0.0009) H-2(β) \rightarrow L(β) 1210.10 (0.0003) H-3(β) \rightarrow L(β)	572

References

- [S1] A. Winter, A. M. J. van den Berg, R. Hoogenboom, G. Kickelbick and U. S. Schubert, *Synthesis*, 2006, 2873-2878.
- [S2] E. C. Constable and A. M. W. C. Thompson, *Chem. Soc. Dalton. Trans.* 1994, **9**, 1409-1418.
- [S3] Y. Liu, H-J. Zhang, Y. Lu, Y-Q. Cai and X-L. Liu, *Green Chem.* 2007, **9**, 1114–1119.
- [S4] E-Y. Choi, L. D. DeVries, R. W. Novotny, C. Hu and W. Choe, *Cryst. Growth Des.* 2010, **10**, 171-176.